Editors' Suggestion | Featured in Physics

Hadronic Light-by-Light Scattering Contribution to the Muon Anomalous Magnetic Moment from Lattice QCD

Thomas Blum,[1,2] Norman Christ,[3] Masashi Hayakawa,[4,5] Taku Izubuchi,[6,2]
Luchang Jin,[1,2,*] Chulwoo Jung,[6] and Christoph Lehner[7,6]

[1]*Physics Department, University of Connecticut, 2152 Hillside Road, Storrs, Connecticut 06269-3046, USA*
[2]*RIKEN BNL Research Center, Brookhaven National Laboratory, Upton, New York 11973, USA*
[3]*Physics Department, Columbia University, New York, New York 10027, USA*
[4]*Department of Physics, Nagoya University, Nagoya 464-8602, Japan*
[5]*Nishina Center, RIKEN, Wako, Saitama 351-0198, Japan*
[6]*Physics Department, Brookhaven National Laboratory, Upton, New York 11973, USA*
[7]*Universität Regensburg, Fakultät für Physik, 93040 Regensburg, Germany*

(Received 18 December 2019; accepted 27 February 2020; published 1 April 2020)

We report the first result for the hadronic light-by-light scattering contribution to the muon anomalous magnetic moment with all errors systematically controlled. Several ensembles using $2+1$ flavors of physical mass Möbius domain-wall fermions, generated by the RBC and UKQCD collaborations, are employed to take the continuum and infinite volume limits of finite volume lattice QED + QCD. We find $a_\mu^{\mathrm{HLbL}} = 7.87(3.06)_{\mathrm{stat}}(1.77)_{\mathrm{sys}} \times 10^{-10}$. Our value is consistent with previous model results and leaves little room for this notoriously difficult hadronic contribution to explain the difference between the standard model and the BNL experiment.

DOI: 10.1103/PhysRevLett.124.132002

Introduction.—The anomalous magnetic moment of the muon is providing an important test of the standard model. The current discrepancy between experiment and theory stands between three and four standard deviations. An ongoing experiment at Fermilab (E989) and one planned at J-PARC (E34) aim to reduce the uncertainty of the BNL E821 value [1] by a factor of four, and similar efforts are underway on the theory side [2–31]. A key part of the latter is to compute the hadronic light-by-light (HLbL) contribution from first principles using lattice QCD [32–38]. Such a calculation, with all errors under control, is crucial to interpret the anticipated improved experimental results [39,40].

The magnetic moment is an intrinsic property of a spin-1/2 particle, and is defined through its interaction with an external magnetic field $\boldsymbol{B}$, $H_{\mathrm{int}} = -\boldsymbol{\mu}\cdot\boldsymbol{B}$. Here

$$\boldsymbol{\mu} = -g\frac{e}{2m}\mathbf{S}, \tag{1}$$

where $\mathbf{S}$ is the particle's spin, q and m are the electric charge and mass, respectively, and g is the Landé g factor. The Dirac equation predicts that $g = 2$, exactly, so any difference from 2 must arise from interactions. Lorentz and gauge symmetries tightly constrain the form of the interactions,

$$\langle\mu(\mathbf{p}')|J_\nu(0)|\mu(\mathbf{p})\rangle = -e\bar{u}(\mathbf{p}')\left(F_1(q^2)\gamma_\nu + i\frac{F_2(q^2)}{4m}[\gamma_\nu,\gamma_\rho]q_\rho\right)u(\mathbf{p}), \tag{2}$$

where J_ν is the electromagnetic current, and F_1 and F_2 are form factors, giving the charge and magnetic moment at zero momentum transfer $[q^2 = (p'-p)^2 = 0]$, or static limit. $u(\mathbf{p})$ and $\bar{u}(\mathbf{p})$ are Dirac spinors. The anomalous part of the magnetic moment is given by $F_2(0)$ alone, and is known as the anomaly,

$$a_\mu \equiv (g-2)/2 = F_2(0). \tag{3}$$

The desired matrix element in (2) is extracted in quantum field theory from a correlation function of fields as depicted in the Feynman diagrams shown in Fig. 1. Here we work in coordinate (Euclidean) space and use lattice QCD for the hadronic part which is intrinsically nonperturbative. QED is treated using the same discrete, finite, lattice as used for the hadronic part, while we remove the spatial zero modes of the photon propagator. This method is called QED_L [41]. It is perturbative with respect to QED, i.e, only diagrams where the hadronic part is connected to the muon by three photons enter the calculation.

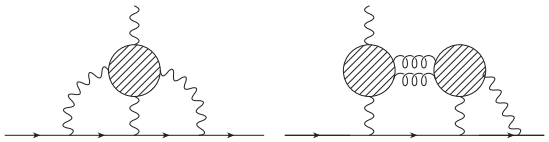

FIG. 1. Leading contributions from hadronic light-by-light scattering to the muon anomaly. The shaded circles represent quark loops containing QCD interactions to all orders. Horizontal lines represent muons. Quark-connected (left) and disconnected (right) diagrams are shown. Ellipsis denote diagrams obtained by permuting the photon contractions with the muons and diagrams with three and four quark loops with photon couplings (See Fig. 3).

QED$_L$ *method.*—Here the muon, photons, quarks, and gluons are treated on a finite, discrete lattice. The method is described in detail in Ref. [33], and the diagrams to be computed are shown in Figs. 2 and 3. It is still not possible to do all of the sums over coordinate space vertices exactly with currently available compute resources. Therefore we resort to a hybrid method where two of the vertices on the hadronic loop(s) are summed stochastically: point source propagators from coordinates x and y are computed, and their sink points are contracted at the third internal vertex z and the external vertex x_{op}. Since the propagators are calculated to all sink points, z and x_{op} can be summed over the entire volume. The sums over vertices x and y are then done stochastically by computing many [O(1000)] random pairs of point source propagators. To do the sampling efficiently, the pairs are chosen with an empirical distribution [42] designed to frequently probe the summand where it is large, less frequently where it is small. Since QCD has a mass gap, we know the hadronic loop is exponentially suppressed according to the distance between any pair of vertices, including $|x-y|$. As we will see, the main contribution comes from distances less than about 1 fm. The muon line and photons are computed efficiently using fast Fourier transforms; however, because they must be calculated many times, the cost is not negligible.

Two additional, but related, parts of the method bear mentioning. First, the form dictated by the right-hand side of Eq. (2) suggests the limit $q \to 0$ is unhelpful since the desired F_2 term is multiplied by 0. Second, in our Monte Carlo lattice QCD calculation the error on the F_2 contribution blows up in this limit. The former is avoided by evaluating the first moment with respect to $\mathbf{x}_{\mathrm{op}}$ at the external vertex and noticing that an induced extra term vanishes exponentially in the infinite volume limit [33]. This moment method allows the direct calculation of the correlation function at $q = 0$, and hence $F_2(0)$. To deal with the second issue, we first recall that it is the Ward identity that guarantees the unwanted term to vanish in the moment method. We thus enforce the Ward identity exactly on a configuration-by-configuration basis [33], i.e., before averaging over gauge fields by inserting the external photon at all possible locations on the quark loop in Fig. 2. This makes the factor of q in Eq. (2) exact for each measurement and not just in the average and reduces the error on $F_2(0)$ significantly. Implementing the above techniques produces an order O(1000)-fold improvement in the statistical error over the original nonperturbative QED method used to compute the hadronic light-by-light scattering contribution [32].

The quark-disconnected diagrams that occur at $O(\alpha^3)$ are shown Fig. 3. All but the upper-leftmost diagram vanish in the SU(3) flavor limit and are suppressed by powers of $m_{u,d} - m_s$, depending on the number of quark loops with a single photon attached. For now we ignore them and concentrate on the leading disconnected diagram which is computed with a method [34] similar to the one described in the first part of this section. To ensure the loops are connected by gluons, explicit vacuum subtraction is required. However, in the leading diagram the moment at x_{op} implies the left-hand loop in Fig. 3 vanishes due to parity symmetry, and the vacuum subtraction is done to reduce noise.

As for the connected case, two point sources (at y and z in Fig. 3) are chosen randomly, and the sink points (at x and x_{op} in Fig. 3) are summed over. We compute M (usually

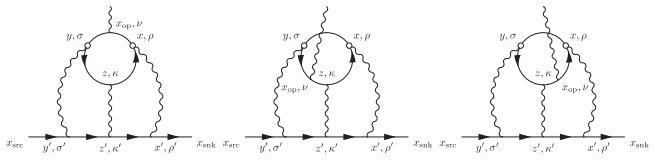

FIG. 2. Connected diagrams. Sums over x and y are computed stochastically. The third internal vertex z and the external vertex x_{op} are summed over exactly. The sums on the muon line are done exactly using fast Fourier transforms. Strong interactions to all orders are not shown.

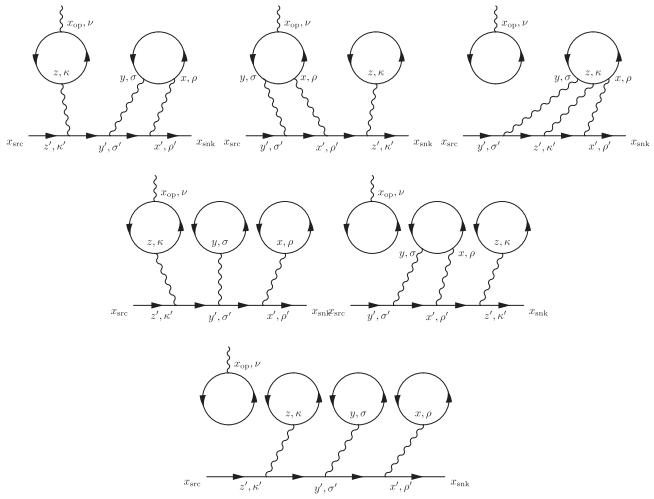

FIG. 3. Disconnected diagrams contributing to the muon anomaly. The top leftmost is the leading one, and does not vanish in the SU(3) flavor limit. Strong interactions to all orders, including gluons connecting the quark loops, are not shown.

TABLE I. $2+1$ flavors of MDWF gauge field ensembles generated by the RBC and UKQCD collaborations [47]. The lattice spacing a, spatial extent L, extra fifth dimension size L_s, muon pion mass m_π, and number of QCD configuration used for the connected and the disconnected diagrams.

	48I	64I	24D	32D	48D	32D fine
a^{-1} (GeV)	1.730	2.359	1.015	1.015	1.015	1.378
a (fm)	0.114	0.084	0.194	0.194	0.194	0.143
L (fm)	5.47	5.38	4.67	6.22	9.33	4.58
L_s	48	64	24	24	24	32
m_π (MeV)	139	135	142	142	142	144
m_μ (MeV)	106	106	106	106	106	106
# meas con	65	43	157	70	8	75
# meas discon	124	105	156	69	0	69

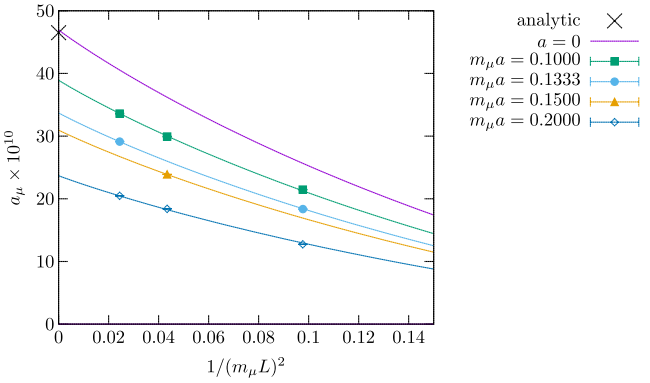

FIG. 4. QED light-by-light scattering contribution from the muon loop to the muon anomaly. The lattice spacing decreases from bottom to top. Solid lines are from a fit using Eq. (4).

$M = 1024$) point source propagators for each configuration. All M^2 combinations are used to perform the stochastic sum over $y - z$. This "M^2 trick" [33,34] is crucial to bring the statistical fluctuations of the disconnected diagram under control (see Section B of the Supplemental Material [43] for more details).

Lattice setup.—The simulation parameters are given in Table I. All particles have their physical masses (isospin breaking for the up and down quark masses is not included). The discrete Dirac operator is known as the (Möbius) domain wall fermion [(M)DWF)] operator. Similarly the discrete gluon action is given by the plaquette plus rectangle Iwasaki gauge action. Additionally, three ensembles with larger lattice spacing employ the dislocation-suppressing-determinant-ratio (DSDR) to soften explicit chiral symmetry breaking effects for MDWFs [44]. We use all mode averaging [45] and multigrid Lanczos [46] techniques to speed up the fermion propagator generation.

The muons and photons take discrete free-field forms. The muons are DWFs with infinite size in the extra fifth dimension, and the photons are noncompact in the Feynman gauge. In the latter all modes with $\mathbf{q} = 0$ are dropped, a finite volume formulation of QED known as QED$_L$ [41].

Results.—Before moving to the hadronic case, the method was tested in pure QED [33]. Results for several lattice spacings and box sizes are shown in Fig. 4. The systematic uncertainties are large, but under control. Note that the finite volume errors are polynomial in $1/L$ and not exponential, due to the photons which interact over a long range. The data are well fit to the form

$$a_\mu(L,a) = a_\mu\left(1 - \frac{b_2}{(m_\mu L)^2} + \frac{b_3}{(m_\mu L)^3}\right) \times (1 - c_1(m_\mu a)^2 + c_2(m_\mu a)^4). \quad (4)$$

The continuum and infinite volume limit is $F_2(0) = 46.9(2)_{\text{stat}} \times 10^{-10}$ for the case where the lepton mass in the loop is the same as the muon mass, which is quite consistent with the well-known perturbative value [48], 46.5×10^{-10}.

Our physical point calculation [34] started on the 48^3, $a^{-1} = 1.730$ GeV, Iwasaki ensemble listed in the first column of Table I, for which we found $a_\mu^{\text{con}} = 11.60(0.96)_{\text{stat}} \times 10^{-10}$, $a_\mu^{\text{discon}} = -6.25(0.80)_{\text{stat}} \times 10^{-10}$, and $a_\mu^{\text{tot}} = 5.35(1.35)_{\text{stat}} \times 10^{-10}$ for the connected, leading disconnected, and total HLbL contributions to the muon anomaly, respectively. The errors quoted are purely statistical. We have since improved the statistics on the leading disconnected diagram with measurements on 59 additional configurations, and the contribution becomes $-6.15(55) \times 10^{-10}$. Since then we have computed on several additional ensembles in order to take the continuum and infinite volume limits (see Tab. I).

The results are displayed in Fig. 5 along with curves obtained with the following equation:

$$a_\mu(L,a^I,a^D) = a_\mu\left(1 - \frac{b_2}{(m_\mu L)^2} - c_1^I(a^I\,\text{GeV})^2 - c_1^D(a^D\,\text{GeV})^2 + c_2^D(a^D\,\text{GeV})^4\right) \quad (5)$$

where a^I, a^D represent the lattice spacings for the Iwasaki and I-DSDR ensembles, respectively. For the Iwasaki ensembles, we define the variable a^D to be zero and vice versa. Therefore the lattice spacing is always equal to $a = a^I + a^D$. We allow different a^2 coefficients for the Iwasaki and I-DSDR ensembles as the gauge actions are different. The lattice spacings for the I-DSDR ensembles are not small enough to allow us to ignore the a^4 effects, and therefore we include them in the fit. As we only have two lattice spacings for the I-DSDR ensembles, with both a^2 and a^4 effects unknown, we cannot extrapolate to the continuum just with the I-DSDR ensembles. Therefore, based on this fit form, the continuum limit is obtained from the two Iwasaki ensembles, and the I-DSDR ensembles are used to obtain the volume dependence only. In particular,

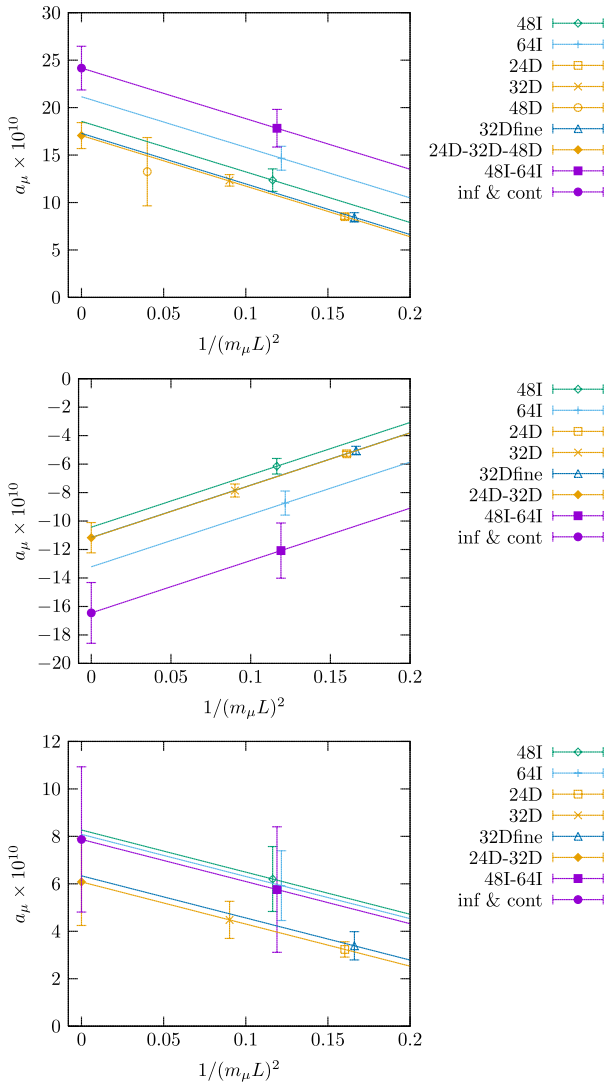

FIG. 5. Infinite volume extrapolation. Connected (top), disconnected (middle), and total (bottom). We have use the hybrid method to calculate the continuum limit for the connected contribution.

the 32Dfine ensemble does not affect the fitted a_μ at all. It only helps to determine the parameter c_2^D, which provides evidence for the size of the potential $\mathcal{O}(a^4)$ systematic errors. We find for the connected, disconnected, and total contributions, $a_\mu^{\rm con} = 23.76(3.96)_{\rm stat}(4.88)_{\rm sys} \times 10^{-10}$, $a_\mu^{\rm discon} = -16.45(2.13)_{\rm stat}(3.99)_{\rm sys} \times 10^{-10}$, $a_\mu^{\rm tot} = 7.47(4.24)_{\rm stat}(1.64)_{\rm sys} \times 10^{-10}$, respectively. For the total contribution, we fit the total contribution for each ensemble, which is slightly different from the sum of the fitted results from the connected and the disconnected parts. Notice there is a large cancellation between the connected and disconnected diagrams that persists for $a \to 0$ and $L \to \infty$, so even though the individual contributions are relatively well resolved, the total is not. The cancellation is expected since hadronic light-by-light scattering at long distance is dominated by the π^0 which contributes to both diagrams, but with opposite sign [36,49,50]. Notice also that the a^2 and $1/L^2$ corrections are individually large but also tend to cancel in the sum.

The systematic errors mostly result from the higher order discretization and finite volume effects which are not included in the fitting formula Eq. (5). We therefore estimate the errors through the change of the results after adding a corresponding term in the fitting formula. For $\mathcal{O}(1/L^3)$, we add another $1/(m_\mu L)^3$ term with the same coefficient as the $1/(m_\mu L)^2$ term. For $\mathcal{O}(a^4)$ effects, we add an a^4 term also for the Iwasaki ensembles with coefficient similar to the I-DSDR ensembles. For $\mathcal{O}[a^2 \log(a^2)]$ effects, we multiply the discretization effect terms in Eq. (5) by $[1 - (\alpha_S/\pi)\log(a^2\,\mathrm{GeV})]$. For $\mathcal{O}(a^2/L)$, we multiply the discretization effect terms in Eq. (5) by $[1 - 1/(m_\mu L)]$. In addition, for the only two contributions which we have not included in the present HLbL calculation: (i) strange quark contribution to the connected diagrams; (ii) subleading disconnected diagrams' contribution. We have performed lattice calculations with the QED$_\infty$ approach [51] on the 24D ensemble to estimate the systematic errors. These systematic errors are added in quadrature and summarized in Table II. In the Supplemental Material [43], these systematic errors are discussed in more detail.

While the large relative error on the total is a bit unsatisfactory, we emphasize that our result represents an important estimate on the hadronic light-by-light scattering contribution to the muon anomaly, with all systematic errors controlled. It appears that this contribution cannot bring the standard model and the E821 experiment in agreement.

In fact we can do even a bit better with the data on hand. As seen in Fig. 6, which shows the cumulative sum of all contributions up to a given separation of the two sampled currents in the hadronic loop, the total connected contribution saturates at a distance of about 1 fm for all ensembles. This suggests the region $r \gtrsim 1$ fm adds mostly noise and little signal, and the situation gets worse in the

TABLE II. Central value and various systematic errors. Numbers in parentheses are statistical error for the corresponding values.

	con	discon	tot
a_μ	23.76(3.96)	−16.45(2.13)	7.47(4.24)
sys $\mathcal{O}(1/L^3)$	2.34(0.41)	1.72(0.32)	0.83(0.56)
sys $\mathcal{O}(a^4)$	0.83(0.53)	0.71(0.28)	0.96(0.94)
sys $\mathcal{O}[a^2 \log(a^2)]$	0.21(0.18)	0.25(0.09)	0.03(0.17)
sys $\mathcal{O}(a^2/L)$	4.18(2.37)	3.49(1.37)	0.86(2.20)
sys strange con	0.30	0	0.30
sys subdiscon	0	0.50	0.50
sys all	4.88(2.17)	3.99(1.29)	1.64(1.15)

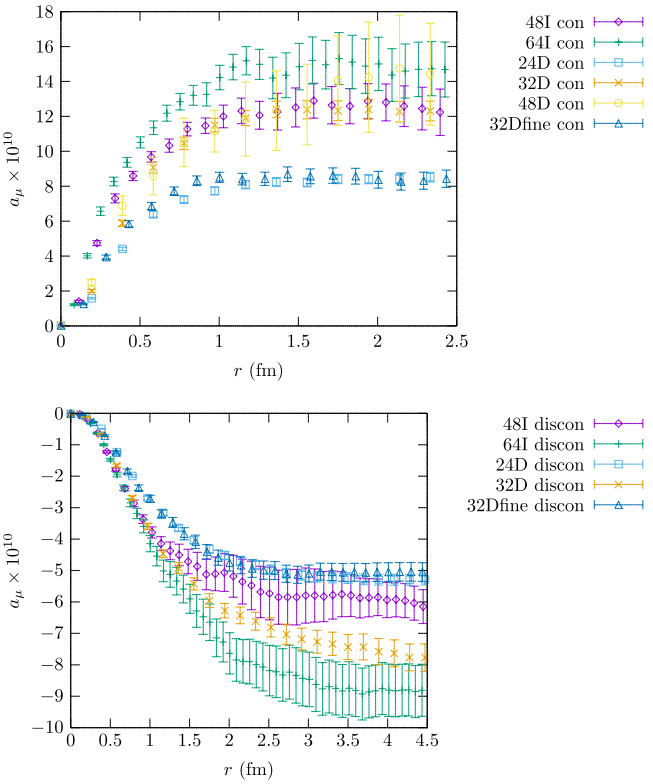

FIG. 6. Cumulative contributions to the muon anomaly, connected (upper) and disconnected (lower). r is the distance between the two sampled currents in the hadronic loop (the other two currents are summed exactly) and the horizontal axis is the cumulative contributions from r and below: 24^3 IDSDR (squares), 24^3 IDSDR (squares), 32^3 IDSDR (crosses), 48^3 Iwasaki (diamonds), and 64^3 Iwasaki (plusses).

limits. A more accurate estimate can be obtained by taking the continuum limit for the sum up to $r = 1$ fm, and above that by taking the contribution from the relatively precise 48^3 ensemble. We include a systematic error on this long distance part since it is not extrapolated to $a = 0$. The infinite volume limit is taken as before. This hybrid procedure yields $a_\mu^{\mathrm{con}} = 24.16(2.30)_{\mathrm{stat}}(5.11)_{\mathrm{sys}} \times 10^{-10}$, with a statistical error that is roughly $2\times$ smaller and the additional $\mathcal{O}(a^2)$ systematic error from the hybrid procedure is only 0.20×10^{-10}. Unfortunately a similar procedure for the disconnected diagram is not reliable, as can be seen in the lower panel of Fig. 6. The cumulative plots do not reach plateaus around 1 fm, but instead tend to fall significantly up to 2 fm, or more. Once the cut moves beyond 1 fm it is no longer effective. The different behavior between the two stems from the different sampling strategies used for each [33]. Using the improved connected result, we find our final result for QED_L,

$$a_\mu^{\mathrm{tot}} = 7.87(3.06)_{\mathrm{stat}}(1.77)_{\mathrm{sys}} \times 10^{-10}, \tag{6}$$

where the error is mostly statistical. We also include all systematic errors added in quadrature, including the hybrid $\mathcal{O}(a^2)$ error of the connected diagram. The systematic errors are summarized in Table III.

TABLE III. Central value and various systematic errors, use the hybrid continuum limit for the connected diagrams. Numbers in parentheses are statistical error for the corresponding values.

	con	discon	tot
a_μ	24.16(2.30)	−16.45(2.13)	7.87(3.06)
sys hybrid $\mathcal{O}(a^2)$	0.20(0.45)	0	0.20(0.45)
sys $\mathcal{O}(1/L^3)$	2.34(0.41)	1.72(0.32)	0.83(0.56)
sys $\mathcal{O}(a^4)$	0.88(0.31)	0.71(0.28)	0.95(0.92)
sys $\mathcal{O}(a^2 \log(a^2))$	0.23(0.08)	0.25(0.09)	0.02(0.11)
sys $\mathcal{O}(a^2/L)$	4.43(1.38)	3.49(1.37)	1.08(1.57)
sys strange con	0.30	0	0.30
sys subdiscon	0	0.50	0.50
sys all	5.11(1.32)	3.99(1.29)	1.77(1.13)

Summary and outlook.—We have presented results for the hadronic light-by-light scattering contribution to the muon $g-2$ from Lattice QCD + QED calculations with all errors under control. Large discretization and finite volume corrections are apparent but under control, and the value in the continuum and infinite volume limits is compatible with previous model and dispersive treatments, albeit with a large statistical error. Despite the large error, which results after a large cancellation between quark-connected and disconnected diagrams, our calculation suggests that light-by-light scattering can not be behind the approximately 3.7 standard deviation discrepancy between the standard model and the BNL experiment E821. Future calculations will reduce the error significantly. The calculations presented here strengthen the much anticipated test of the standard model from the new experiments at Fermilab and J-PARC, with the former planning to announce first results soon.

tWe would like to thank our RBC and UKQCD collaborators for helpful discussions and critical software and hardware support. This work is partially supported by the U.S. Department of Energy. T. B. and L. C. J. are supported by U.S. DOE Grant No. DE-SC0010339. N. C. is supported by U.S. DOE Grant No. DE-SC0011941. M. H. is supported in by Japan Grants-in-Aid for Scientific Research, No. 16K05317. T. I. and C. L. are supported in part by U.S. DOE Contract No. DESC0012704(BNL). T. I. is also supported by JSPS KAKENHI Grants No. JP26400261 and No. JP17H02906. C. L. is also supported by a DOE Office of Science Early Career Award. We developed the computational code based on the Columbia Physics System (CPS) and Grid [52]. Computations were performed mainly under the ALCC Program of the U.S. DOE on the Blue Gene/Q Mira computer at the Argonne Leadership Class Facility, a DOE Office of Science Facility supported under Contract No. DE-AC02-06CH11357. We gratefully acknowledge computer resources at the Oakforest-PACS supercomputer system at Tokyo University, partly through

the HPCI System Research Project (hp180151, hp190137), the BNL SDCC computer clusters at Brookhaven National Lab as well as computing resources provided through USQCD at the Brookhaven and Jefferson Labs.

*ljin.luchang@gmail.com

[1] G. W. Bennett *et al.* (Muon g-2 Collaboration), Phys. Rev. D **73**, 072003 (2006).
[2] C. Aubin, T. Blum, C. Tu, M. Golterman, C. Jung, and S. Peris, Phys. Rev. D **101**, 014503 (2020).
[3] T. Blum, P. A. Boyle, T. Izubuchi, L. Jin, A. Jüttner, C. Lehner, K. Maltman, M. Marinkovic, A. Portelli, and M. Spraggs, Phys. Rev. Lett. **116**, 232002 (2016).
[4] C. Lehner *et al.* (USQCD Collaboration), Eur. Phys. J. A **55**, 195 (2019).
[5] C. T. H. Davies *et al.* (Fermilab Lattice and LATTICE-HPQCD and MILC Collaborations), Phys. Rev. D **101**, 034512 (2020).
[6] D. Giusti, V. Lubicz, G. Martinelli, F. Sanfilippo, and S. Simula, Phys. Rev. D **99**, 114502 (2019).
[7] G. Colangelo, M. Hoferichter, M. Procura, and P. Stoffer, Phys. Rev. Lett. **118**, 232001 (2017).
[8] G. Colangelo, M. Hoferichter, M. Procura, and P. Stoffer, J. High Energy Phys. 09 (2015) 074.
[9] G. Colangelo, M. Hoferichter, M. Procura, and P. Stoffer, J. High Energy Phys. 04 (2017) 161.
[10] G. Colangelo, F. Hagelstein, M. Hoferichter, L. Laub, and P. Stoffer, arXiv:1910.11881.
[11] G. Colangelo, F. Hagelstein, M. Hoferichter, L. Laub, and P. Stoffer, arXiv:1910.13432.
[12] M. Hoferichter, B. L. Hoid, B. Kubis, S. Leupold, and S. P. Schneider, Phys. Rev. Lett. **121**, 112002 (2018).
[13] F. Hagelstein and V. Pascalutsa, Phys. Rev. Lett. **120**, 072002 (2018).
[14] P. Masjuan and P. Sanchez-Puertas, Phys. Rev. D **95**, 054026 (2017).
[15] M. Davier, A. Hoecker, B. Malaescu, and Z. Zhang, arXiv:1908.00921.
[16] M. Hoferichter, B. L. Hoid, and B. Kubis, J. High Energy Phys. 08 (2019) 137.
[17] A. Gérardin, H. B. Meyer, and A. Nyffeler, Phys. Rev. D **94**, 074507 (2016).
[18] A. Gérardin, M. Ce, G. vonHippel, B. Horz, H. B. Meyer, D. Mohler, K. Ottnad, J. Wilhelm, and H. Wittig, Phys. Rev. D **100**, 014510 (2019).
[19] E. Shintani and Y. Kuramashi (PACS Collaboration), Phys. Rev. D **100**, 034517 (2019).
[20] G. Colangelo, M. Hoferichter, and P. Stoffer, J. High Energy Phys. 02 (2019) 006.
[21] G. Colangelo, M. Hoferichter, B. Kubis, M. Procura, and P. Stoffer, Phys. Lett. B **738**, 6 (2014).
[22] D. Giusti, F. Sanfilippo, and S. Simula, Phys. Rev. D **98**, 114504 (2018).
[23] T. Blum, P. A. Boyle, V. Gülpers, T. Izubuchi, L. Jin, C. Jung, A. Jüttner, C. Lehner, A. Portelli, and J. T. Tsang (RBC and UKQCD Collaborations), Phys. Rev. Lett. **121**, 022003 (2018).
[24] B. Chakraborty, C. T. H. Davies, C. DeTar, A. X. El-Khadra, E. Gamiz *et al.* (Fermilab Lattice and LATTICE-HPQCD and MILC Collaborations), Phys. Rev. Lett. **120**, 152001 (2018).
[25] S. Borsanyi *et al.* (Budapest-Marseille-Wuppertal Collaboration), Phys. Rev. Lett. **121**, 022002 (2018).
[26] T. Izubuchi, Y. Kuramashi, C. Lehner, and E. Shintani (PACS Collaboration), Phys. Rev. D **98**, 054505 (2018).
[27] B. Chakraborty, C. T. H. Davies, J. Koponen, G. P. Lepage, and R. S. Van de Water, Phys. Rev. D **98**, 094503 (2018).
[28] A. Keshavarzi, D. Nomura, and T. Teubner, Phys. Rev. D **97**, 114025 (2018).
[29] M. Hoferichter, B. L. Hoid, B. Kubis, S. Leupold, and S. P. Schneider, J. High Energy Phys. 10 (2018) 141.
[30] T. Blum, Phys. Rev. Lett. **91**, 052001 (2003).
[31] M. Knecht, S. Peris, M. Perrottet, and E. de Rafael, Phys. Rev. Lett. **83**, 5230 (1999).
[32] T. Blum, S. Chowdhury, M. Hayakawa, and T. Izubuchi, Phys. Rev. Lett. **114**, 012001 (2015).
[33] T. Blum, N. Christ, M. Hayakawa, T. Izubuchi, L. Jin, and C. Lehner, Phys. Rev. D **93**, 014503 (2016).
[34] T. Blum, N. Christ, M. Hayakawa, T. Izubuchi, L. Jin, C. Jung, and C. Lehner, Phys. Rev. Lett. **118**, 022005 (2017).
[35] N. Asmussen, J. Green, H. B. Meyer, and A. Nyffeler, *Proc. Sci.*, LATTICE2016 (2016) 164.
[36] A. Gérardin, J. Green, O. Gryniuk, G. von Hippel, H. B. Meyer, V. Pascalutsa, and H. Wittig, Phys. Rev. D **98**, 074501 (2018).
[37] J. Green, O. Gryniuk, G. von Hippel, H. B. Meyer, and V. Pascalutsa, Phys. Rev. Lett. **115**, 222003 (2015).
[38] H. B. Meyer and H. Wittig, Prog. Part. Nucl. Phys. **104**, 46 (2019).
[39] H. Davoudiasl and W. J. Marciano, Phys. Rev. D **98**, 075011 (2018).
[40] A. Crivellin, M. Hoferichter, and P. Schmidt-Wellenburg, Phys. Rev. D **98**, 113002 (2018).
[41] M. Hayakawa and S. Uno, Prog. Theor. Phys. **120**, 413 (2008).
[42] We continue to use the distribution as described in our previous Letter [34]. The same distribution is used for all our ensembles.
[43] See the Supplemental Material at http://link.aps.org/supplemental/10.1103/PhysRevLett.124.132002 for details of QED test, point sampling, and systematic error estimation.
[44] D. Renfrew, T. Blum, N. Christ, R. Mawhinney, and P. Vranas, *Proc. Sci.*, LATTICE2008 (2008) 048.
[45] E. Shintani, R. Arthur, T. Blum, T. Izubuchi, C. Jung, and C. Lehner, Phys. Rev. D **91**, 114511 (2015).
[46] M. A. Clark, C. Jung, and C. Lehner, EPJ Web Conf. **175**, 14023 (2018).
[47] T. Blum, P. A. Boyle, N. H. Christ, J. Frison, N. Garron *et al.* (RBC and UKQCD Collaborations), Phys. Rev. D **93**, 074505 (2016).
[48] S. Laporta and E. Remiddi, Phys. Lett. B **265**, 182 (1991).
[49] J. Bijnens and J. Relefors, J. High Energy Phys. 09 (2016) 113.
[50] L. Jin, T. Blum, N. Christ, M. Hayakawa, T. Izubuchi, C. Jung, and C. Lehner, *Proc. Sci.*, LATTICE2016 (2016) 181.
[51] T. Blum, N. Christ, M. Hayakawa, T. Izubuchi, L. Jin, C. Jung, and C. Lehner, Phys. Rev. D **96**, 034515 (2017).
[52] https://github.com/paboyle/Grid.